Hindawi
International Journal of Energy Research
Volume 2024, Article ID 6632582, 12 pages
https://doi.org/10.1155/2024/6632582

Research Article

CFD Analysis of a Latent Thermal Storage System (PCM) for Integration with an Air-Water Heat Pump

Piera Di Prima,[1,2] Michele Santovito,[3] and Davide Papurello [1,4]

[1]*Department of Energy (DENERG), Politecnico di Torino, Corso Duca degli Abruzzi, 24, 10129 Turin, Italy*
[2]*Department of Applied Science and Technology (DISAT), Politecnico di Torino, Corso Duca degli Abruzzi, 24 10100 Turin, Italy*
[3]*i-TES, Thermal Energy Storage, Via Gioacchino Quarello, 15, 10135 Turin, Italy*
[4]*Energy Center, Politecnico di Torino, Via Paolo Borsellino 38/16, 10138 Turin, Italy*

Correspondence should be addressed to Davide Papurello; davide.papurello@polito.it

Received 6 December 2023; Revised 24 January 2024; Accepted 14 March 2024; Published 25 March 2024

Academic Editor: Mahendra Bhadu

Heat pumps driven by sustainable electricity sources have been identified as a technology that can contribute to reduce carbon dioxide emissions. Furthermore, a heat pump can also provide energy savings when combined with a thermal energy storage system. Heat pumps can optimize their efficiency by accumulating thermal energy during periods of lower electricity demand, resulting in shorter operational durations and decreased overall energy consumption. In this work, the combination of a latent heat storage system with an air-water heat pump has been numerically analysed and experimentally tested. A phase change material (PCM) heat exchanger with an immersed plate was designed using a 3D CFD model (COMSOL Multiphysics®). The heat exchanger configuration with six steel plates immersed in the phase change material tank was proposed to enhance heat transfer in the storage system. The developed model is validated against experimental data from a real case study, demonstrating a maximum error of approximately 3% during the discharging phase. Additionally, the study explores the effects of different inlet heat transfer fluid temperatures and flow rates on the PCM solidification time.

1. Introduction

The growing energy demand, along with the need to limit the usage of fossil fuels, has hastened the integration of renewable energy resources. However, the discontinuity in renewable energy production and the variation in daily energy demand necessitate the development of efficient and sustainable technologies for energy storage. According to the data reported by the International Energy Agency in the World Energy Outlook 2019, the energy used for heating, domestic hot water production, and summer cooling accounts for 50% of global energy consumption in 2018 and is responsible for 40% of carbon dioxide emissions [1]. In this context, heat pumps are becoming increasingly important as part of the technologies with the most significant long-term potential for reducing CO_2 emissions. Heat pumps extract thermal energy from a low-temperature source using a refrigerant, which, in turn, is compressed to transfer the heat to a higher-temperature sink. Since electricity is needed to compress the refrigerant, the environmental impact of a heat pump is closely tied to the source of the electricity used to power it. The Life Cycle Climate Performance is a well-established method to compare refrigerants and heat pumps in terms of emissions and environmental impact [2]. More frequently, the coefficient of performance (COP) is used to measure the efficiency of a heat pump. It is defined as the ratio of the heat delivered by the device to the electrical energy input required. The value assumed by this indicator is strongly influenced by the operating conditions of the heat pump, the temperature of the heat source, and the indoor heat load. Integrating proper thermal energy storage can contribute to achieving a higher COP, reducing the environmental impact of a heat pump. Heat pumps can operate more efficiently and for shorter durations, minimizing compressor usage and decreasing overall energy consumption by storing thermal energy during periods of lower electricity demand. This optimizes energy use and provides flexibility to align heat pump operation with periods of lower environmental impact and greener energy sources.

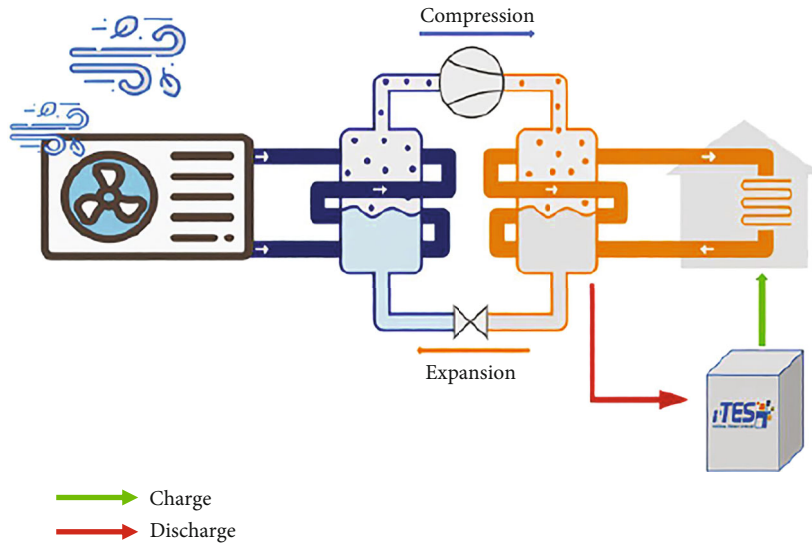

Figure 1: Schematic of the heat pump with a thermal energy storage system.

A latent heat thermal storage system (LHTSS) using phase change materials (PCMs) enables thermal energy storage during phase change at a nearly constant temperature, accumulating higher amounts of heat or cold compared to sensible storage methods. Combining LHTSS with heat pumps synergizes both technologies, leveraging their strengths for energy savings and environmental benefits. This combination enhances the sustainability of heating and cooling processes while optimizing the utilization of renewable energy sources [3–5]. The main drawback of phase change materials is their low thermal conductivity, resulting in slow heat transfer rates. Overcoming this challenge requires the implementation of strategies to enhance heat transfer. Various methods can be employed to address this obstacle, including incorporating additives, using high-conductivity materials, or integrating heat exchanger designs that facilitate more efficient heat exchange [6]. In this study, the storage system was designed with a "plate coil" type immersed exchanger to enhance the PCM heat transfer. Furthermore, a CFD model of the proposed heat exchanger was developed to reproduce the behaviour of the LHTSS when integrated into a domestic air-to-water heat pump for space heating.

Modelling latent heat storage systems is notably more complex than sensible heat storage systems. This complexity arises from the dynamic nature of phase change, during which the heat exchange mechanism undergoes variations over time. During the solidification process, heat transfer is predominantly conductive [7, 8]. Heat conduction predominates in the early phase of the melting process. However, as the phase change progresses, the temperature profile becomes more uniform in the liquid phase, and convective heat transfer becomes more prominent [9]. Moreover, the properties of the PCM vary in three phases: liquid, solid, and liquid-solid (mushy zone).

This work developed the CFD model using COMSOL Multiphysics, considering the evolving mechanisms in latent heat storage systems. The hot water produced by an air-to-water heat pump was used as input for the model. Verification and validation (V&V) procedures were used to estimate numerical and modelling errors and uncertainties in CFD simulations [10], showing that the computational model can accurately reflect physical reality. An experimental study of the thermal storage system combined with an air-to-water heat pump was carried out using an innovative prototype designed and constructed in the laboratory of i-TES srl. This allowed the validation of the model. Finally, the developed model was used to evaluate the effects of different temperatures and flow rates of the inlet water flux on the storage system's performance.

2. Material and Methods

2.1. Heat Pumps for Space Heating Coupled with LHTSS. Air-to-water heat pumps are systems that extract heat from the outdoor air and transfer it to a water-based heating system. During periods of low energy demand, especially in partial load conditions, these heat pumps often experience decreased efficiency, leading to COP than nominal values (e.g., COP nominal = 3.7 for a specific model like Nibe F2040-6 kW from Nibe Industrier, Sweden). The actual COP varies depending on the outside air temperature and the water flow temperature for heating: the higher the former and the lower the latter, the higher the performance of the machine. Factors such as frequent cycling and extended standby periods can further reduce energy efficiency [11]. To mitigate the heat pump's intermittent and inefficient operation, inserting a heat exchanger for the latent thermal storage is possible. In this work, the heat exchanger is placed in series with the hot water production (Figure 1). In this configuration, the heat pump can operate under nominal conditions, channelling the excess thermal energy in the storage tank. The stored energy is then integrated as domestic hot water during the heating phase. This setup optimizes the heat pump's performance, ensuring efficient operation while leveraging thermal storage for improved energy utilization.

Table 1: BioPCM Q42 physical and chemical properties [16].

BioPCM Q42	
Phase transition temperature (°C)	40-42
Total energy storage (latent region) (kJ/kg)	200-215
Thermal conductivity (W/mK)	0.15
Relative density (kg/m^3)	820-875 ($T = 25 - 35$°C)
Specific heat (J/gK)	2.50
Viscosity (Pa•s)	0.003

2.2. PCM Selection and Design of the Heat Exchanger. The PCM selection is crucial in ensuring the optimal performance of LHTSS [12]. Phase change materials can be broadly categorized into three major groups: inorganic, organic, and eutectic mixtures. Organic PCMs, especially paraffin, are widely favoured in various applications due to their favourable thermal properties, good chemical stability, and commercial availability. Their reduced flammability and potential for lower volume change during phase transitions make them a preferable choice compared to eutectic mixtures and inorganic PCMs [13]. Among the organic PCMs, paraffins are the most widely used due to their good thermal physical properties, good chemical stability, and commercial availability [13, 14]. However, they have a significant volume change during the phase change, low thermal conductivity, and relatively low ignition resistance. Compared to paraffinic PCMs, bio-based PCMs show interesting thermal and chemical properties and are significantly less flammable [15]. Based on these considerations, we opted for a bio-based PCM.

The PMC melting temperature is subjected to the specific requirements and constraints of the application. Considering the worst-case scenario for the heat pump operation (lower air temperature in winter in Turin), we obtain an inlet temperature of the water flux in the heat exchanger of around 42°C. Among different bio-based organic PCMs, BioPCM Q42 was selected, which meets the water temperature requirement produced with the heat pump in the worst-case scenario and for economic opportunity dictated by the company i-TES.

The properties of the selected PCM and the melting/solidification phases are described in Table 1. From the differential scanning calorimetry curve of PCM, seen in Figure 2, the phase change temperature ranges are approximately 37-43°C, with a peak temperature of 40°C for the melting process and 38-46°C with a peak temperature of 42°C for the solidification process.

2.3. Design of the LHTSS. The specific design and dimensions of the tank directly impact how efficiently thermal energy is transferred during phase transitions, consequently shaping the duration required for the PCM to undergo melting and ultimately affecting the overall effectiveness of the thermal energy storage [15]. Once the PCM material is selected, an initial estimation of storage size can be derived by considering the amount of energy that the PCM can store. Considering that the energy storage capacity required for this application is approximately 3 kWh, using the material properties in Table 1, we obtained an exploitable volume of 0.062 m^3, corresponding to 54 kg of PCM material.

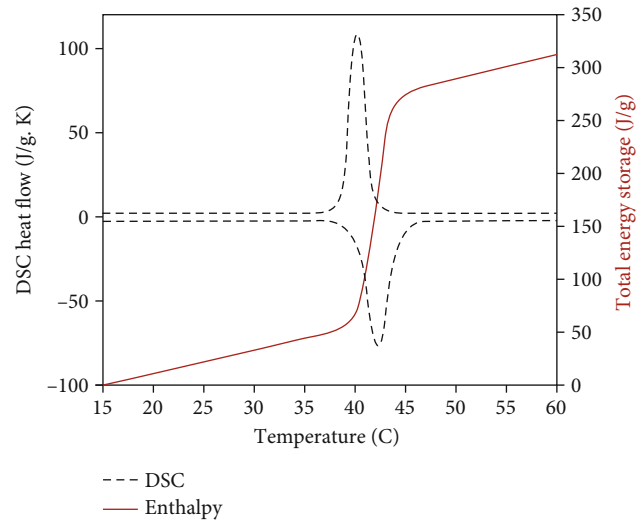

Figure 2: Thermal properties of the PCM obtained with differential scanning calorimetry (DSC) [16].

$$m_{\mathrm{PCM}} = \frac{E_{\mathrm{acc}}}{\Delta H} = 54\,\mathrm{kg},$$
$$V_{\mathrm{PCM}} = \frac{m_{\mathrm{PCM}}}{\rho_{\mathrm{PCM}}} = 0.062\,\mathrm{m}^3. \quad (1)$$

Once the volume is established, it becomes crucial to assess its compatibility with the type of heat exchanger employed [17]. In this work, a series of steel plates have been used to increase the heat exchange area of the storage system as an alternative to the classic configuration with pipes. Considering the geometry of the plates, we opted for a parallelepiped-shaped tank with a square base. The heat exchanger unit obtained in this study comprises an insulated vessel designed to contain the phase change material (PCM). This vessel incorporates six plates made of AISI 304, each with a thickness of 1 mm, serving as the primary components for heat exchange. Figure 3 provides a visual representation of the heat exchanger and one individual plate.

2.4. Experimental Test. For the experimental data collection, a small "private" house was used with a radiator installed to heat a room ($3 \times 4 \times 2.7$ m). To measure the temperature inside the room, a thermometer with an accuracy of ±0.5°C was used (HOBO Pendant MX Water Temperature Data Logger). The heat storage tank, with a volume of

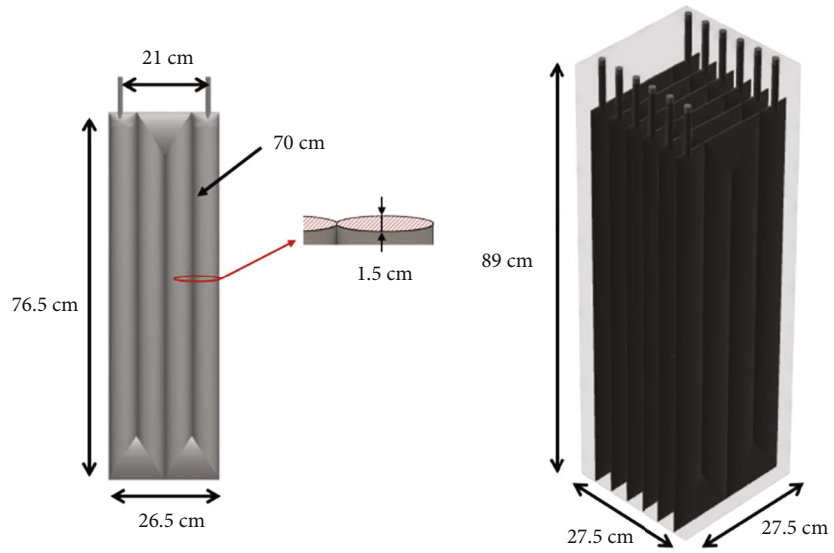

Figure 3: Representation of the PCM heat exchanger and one individual plate with all relevant dimensions.

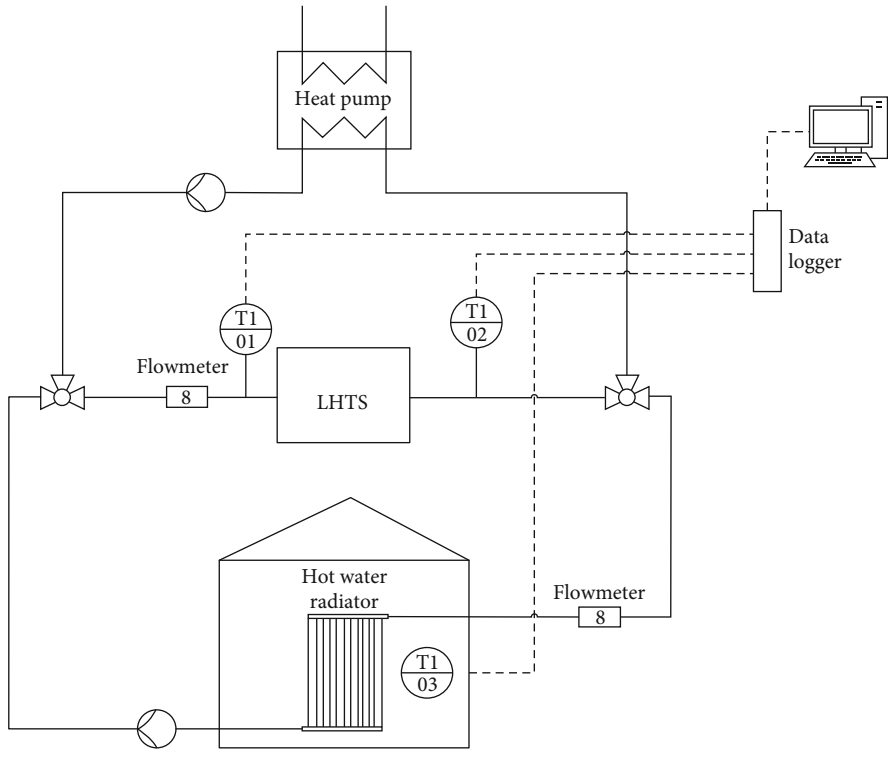

Figure 4: Schematic of the experimental setup.

0.0605 m^3, was connected to the heat pump (Nibe F2040-6 kW) and the radiator (10 elements made of aluminium). At the same time, two thermocouples (type T IEC RS Pro) with an accuracy of ±0.5°C were placed at the inlet and outlet of the storage, respectively. Two flowmeters were used (ES-Flow, Bronkhorst High-Tech BV, the Netherlands). The experimental apparatus was designed to allow the system to be charged and discharged with a constant HTF flow rate and variable temperature (see Figure 4).

3. Mathematical and Numerical Model

The formalisation of isothermal phase change problems is attributed to Austrian physicist Josef Stefan [18]. The model was elaborated considering the interface between solid and liquid phases as a moving boundary during the process where the position of the moving boundary must be determined as a function of time and space [19, 20]. Therefore, the primary challenge in such problems lies in managing a

moving interface involving mass and heat transfer equations strictly dependent on each other. Mathematically, these models are solved using variable grid methods: the solid and the liquid phases are implemented in two separate domains, and the interface between them is continuously tracked over time. A fixed grid approach can be employed to simplify the model and reduce the computational demand. This method employs a single computational domain, applying a unified set of equations. It relies on the physical average of variables using liquid-solid mass and volume fraction [21]. Consequently, in this work, the heat transfer inside the thermal storage was modelled by using a fixed grid model based on the apparent heat capacity approach.

3.1. COMSOL Multiphysics. In this work, a three-dimensional CFD model for the thermal energy storage unit was developed using COMSOL Multiphysics. The geometry of the heat exchanger was generated with Autodesk Fusion 360 before being imported into COMSOL. The CFD model is developed to analyse the solidification processes of the PCM. To reduce the computational cost of the model, the following assumptions are considered:

(1) Each plate interacts only with the portion of PCM that surrounds it, and the flow rate of the heat transfer fluid is equally distributed between the plates

(2) Considering the solidification process, it is possible to neglect the natural convection effect for the PCM, as reported also in other studies [7, 22]

(3) Water is used as heat transfer fluid. Its properties have a very low-temperature dependence. Therefore, they have been directly assumed to be constant

(4) Steady-state laminar flow inside the plates

(5) Homogeneous and isotropic PCM with uniform initial temperature

Using the assumptions reported above, it was possible to reduce the computational domain from the whole heat exchanger to half plate with the proper layer of PCM. Furthermore, Navier-Stokes' equations can be solved by separating the heat exchange problem and the dynamic behaviour of the fluid. Finally, this model treats PCM density as a constant value in all solved equations; this approximation is accurate if changes in actual density are small.

3.2. Governing Equations. To simulate the dynamic behaviour of the water flow within metal plates, it should be considered together with the continuity equation and the Navier-Stokes equation. The first one is for the mass conservation, while the second one is for the momentum conservation. The continuity equation is expressed as follows:

$$\nabla \bullet \vec{u} = 0, \tag{2}$$

where $\vec{u}$ is the velocity vector of the fluid.

Under the hypotheses of incompressible, homogeneous, and Newtonian flow, and not considering turbulence models, the Navier-Stokes equations are expressed by the following:

$$\rho \frac{\partial \vec{u}}{\partial t} + \rho\left(\vec{u} \cdot \nabla\right)\vec{u} = -\nabla p + \mu \nabla^2 \vec{u}, \tag{3}$$

where ρ and μ are the density and the viscosity of the water, respectively, and p is the pressure in the fluid. These equations are solved by imposing *no-slip* conditions at the wall of the plates.

The complete energy equation is solved using the velocities found in equations (2) and (3). This represents the convective heat transfer mechanism that occurs in heat exchanger plates. The convective heat transfer is described by the following:

$$\rho c_p \frac{\partial T}{\partial t} + \rho c_p \vec{u} \cdot \nabla T = \nabla \cdot (k \nabla T), \tag{4}$$

where c_p and k are the specific heat and the thermal conductivity of the material, respectively, and T is the temperature. Since this model is used only to simulate the solidification process, as stated before, the convection in the PCM is neglected. Thus, in the rest of the LHTSS, the heat transfer is only by conduction. The equation to be solved is given by the following:

$$\rho c_p \frac{\partial T}{\partial t} = \nabla \cdot (k \nabla T). \tag{5}$$

This equation is solved assuming that all the outside walls are thermally insulated.

The boundary condition of the highly conductive layer is applied to account for in-plane heat flux in the heat exchanger plates:

$$-\vec{n} \bullet (-k \nabla T) = -\nabla_\tau \bullet (-d_{\text{hcl}} k_{\text{hcl}} \nabla_\tau T), \tag{6}$$

where d_{hcl} and k_{hcl} are the layer thickness and conductivity, respectively, and ∇_τ is the tangential derivative.

The apparent heat capacity method was applied to study the phase change process inside the PCM. This approach increases the material's heat capacity within the melting region to ensure that the additional energy needed to heat the material corresponds to the latent heat [8]. From a mathematical point of view, it is possible to write the following equation:

$$\int_{T_s}^{T_l} c_{\text{app}} dT = \int_{T_s}^{T_l} c(T) dT + \lambda, \tag{7}$$

where "c_{app}" is the apparent heat capacity, λ is the latent heat, and T_l and T_s are the temperature of the solid and liquid phases, respectively. In this expression, $T_s = T_{\text{pc}} - dT$ and $T_l = T_{\text{pc}} + dT$, where dT is the average value of the phase transition temperature (T_{pc}). During this temperature interval, the material phase is represented by a smoothed

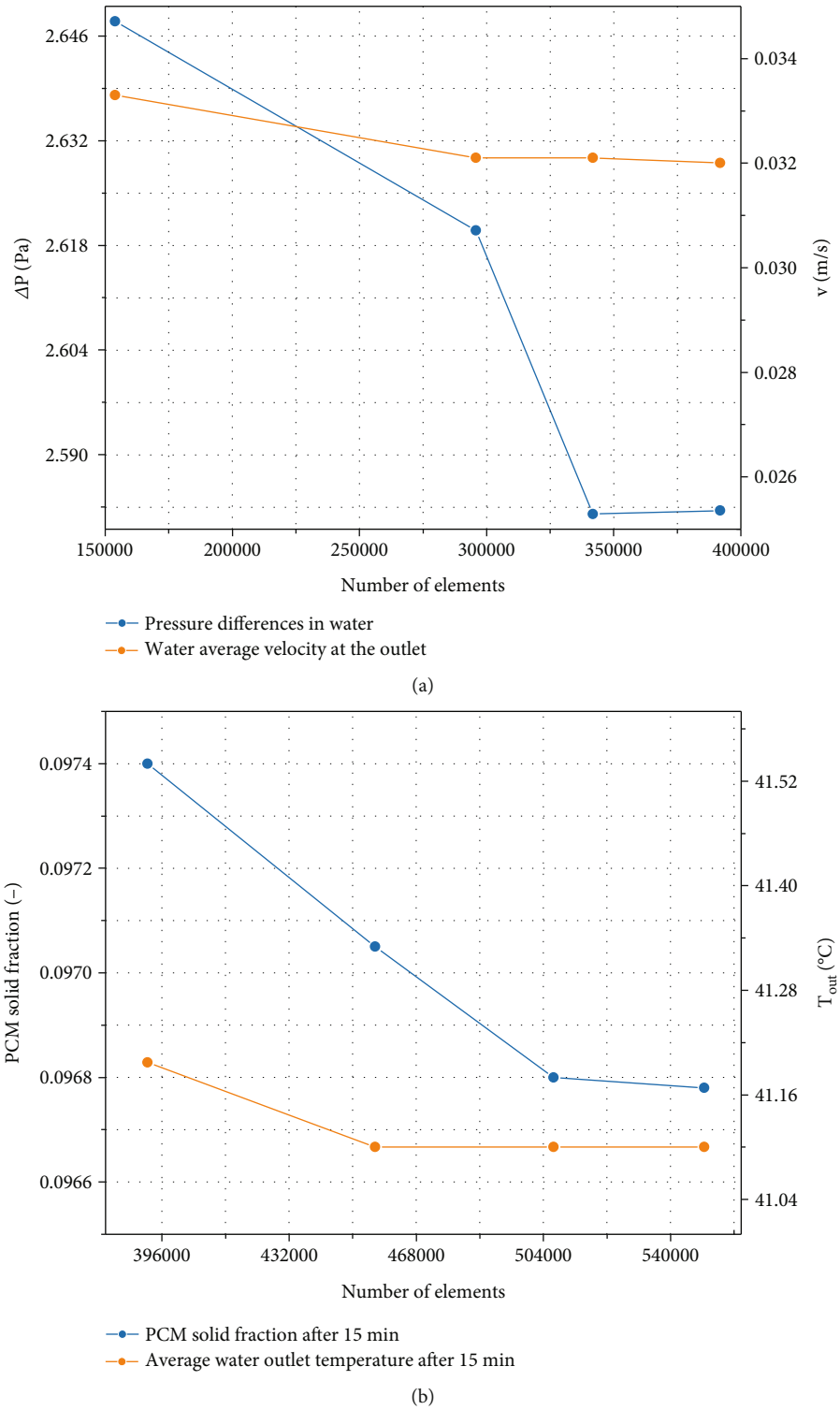

Figure 5: Sensitivity study (a) of the fluid dynamics problem and (b) of the heat transfer problem.

function, θ, which denotes the fraction of phase before the transition and is equal to 1 for $T < T_s$ and to 0 for $T > T_l$. Using this function, the enthalpy during the phase transition is expressed as follows:

$$H = \frac{1}{\rho}(\theta\rho_s H_s + (1-\theta)\rho_l H_l), \tag{8}$$

where the density ρ is given by the following:

$$\rho = \theta\rho_s + (1-\theta)\rho_l. \tag{9}$$

Differentiating the enthalpy concerning temperature and after some transformation, the specific heat capacity during

the phase transition becomes

$$c_{\text{app}} = \frac{1}{\rho}\left(\theta\rho_s c_s + (1-\theta)\rho_l c_l\right) + (H_s - H_l)\frac{d\alpha_{\text{pc}}}{dT}. \quad (10)$$

Here, α_{pc} is the mass fraction defined as follows:

$$\alpha_{\text{pc}} = \frac{1}{2}\frac{(1-\theta)\rho_l c_l - \theta\rho_s c_s}{\rho}. \quad (11)$$

Integrating the last term of equation (10) between T_s and T_l, we obtain the latent heat λ.

3.3. Meshing Dependency and Model Validation. Any results obtained from the CFD analysis must be examined and validated through a proper or simplified experimental test before accepting the results. Therefore, it is appropriate to define procedures to assess errors and uncertainties. The American Society of Mechanical Engineers (ASME) [23] has developed methods to identify the correctness of a computational fluid dynamics model. The verification process will be addressed in the mesh independence study. Ultimately, the numerical model is validated by comparing it with experimental data obtained from the prototype of the LHTSS.

3.3.1. Meshing Dependency. Optimal mesh selection is crucial for obtaining reliable results from numerical models. In this study, an unstructured tetrahedral mesh was employed, allowing for the generation of elements with different sizes adapted to the geometric structure of the component. The mesh independence study is aimed at determining the minimum number of elements that ensure adequate reliability of the results. The formal method for checking mesh independence involves plotting a curve of a critical result parameter at a specific location against the number of cells in the mesh. It is generally recommended to perform at least three simulations to assess the convergence pattern and establish the minimum number of elements that guarantee reliable results. Given the multiphysical nature of the problem, the convergence analysis was performed at two levels. The sensitivity study was conducted on water outlet velocity and pressure drop for the fluid dynamics aspect. On the other hand, for the heat transfer, the independence study was conducted on the outlet water temperature and the solid fraction of PCM after 15 minutes to capture the initial stage of the phase transition. Results for different meshes are reported in Figure 5.

The analysis reveals that the average speed remains nearly constant with increasing mesh elements. In contrast, there is a significant variation in ΔP for the first two meshes, stabilizing to an almost constant value in the last two meshes. Starting from the last mesh, the sensitivity study was conducted on the thermal variables. Considering the simulation time, the CFD model with 507063 elements is deemed more suitable for validation against experimental results.

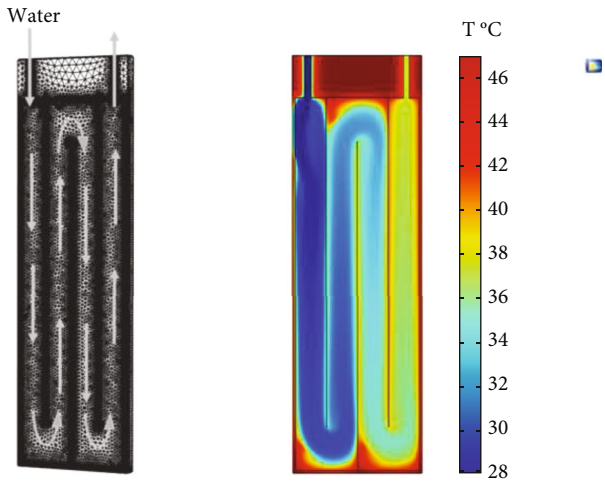

Figure 6: Meshing and temperature profile of the PCM heat exchanger during the discharge phase.

4. Results

4.1. Model Validation. The discharge phase was modelled for the heat exchanger with PCM designed above connected to the air-water heat pump. Results are reported in Figure 6.

To validate the numerical model, the trend of the average temperature of the water at the outlet of the LHTSS was reported and compared with the experimental results. The water mass flow for the two simulations and during the experiment is constant and fixed at around 1 L/min. The inlet temperatures, on the other hand, are different. The inlet temperature of the HTF recorded in April is higher than that recorded in March due to the climatic conditions prevailing each day. The comparison between numerical curves and the experimental data obtained on two different days is shown in Figure 7. The comparison demonstrates a satisfactory agreement between the simulation and experimental results, evident in both the shape of the curves and the quantitative values. The absolute errors assessed during the discharge process exhibit maximum and average values of 1.15°C and 0.69°C, respectively. Based on the obtained results, it can be confidently stated that the constructed model effectively predicts the thermal behaviour of the prototype during the discharge phase, exhibiting a maximum error of 3%. This indicates a high level of accuracy and reliability in capturing the system's thermal dynamics in the simulated conditions.

4.2. Dependency Study. The melting and solidification rates of PCM are influenced mainly by two operating conditions: mass flow rate and inlet temperature of HTF [24, 25]. In this section, the developed and validated 3D CFD model is used to predict and analyse the effects of these parameters on the discharge of the latent heat storage unit.

4.2.1. Flow Rate Dependency. The thermal performance of a latent heat storage system can be enhanced through various strategies, including the incorporation of fins, metal matrices, and dispersion of high-conductivity nanomaterials into

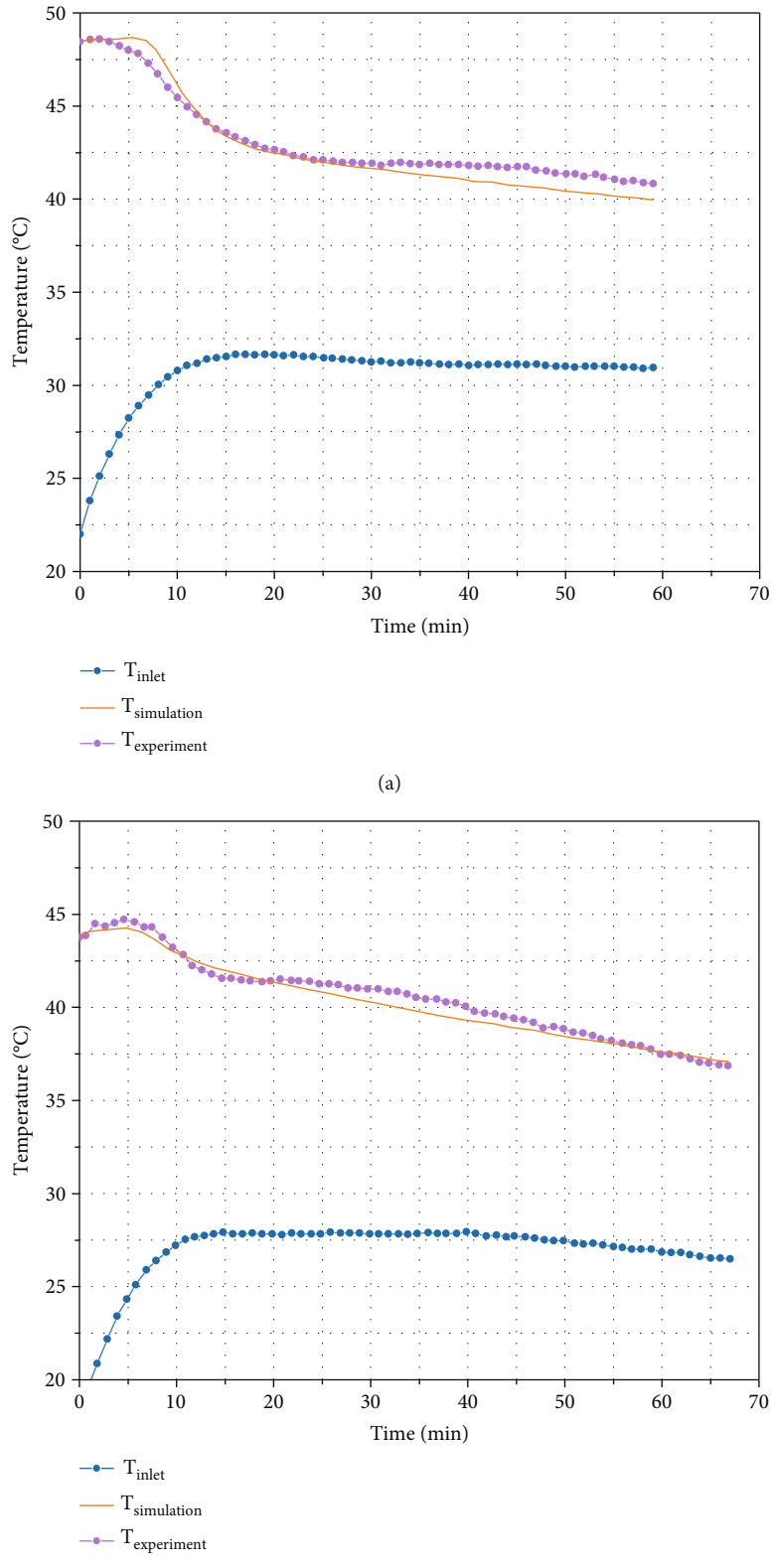

Figure 7: Comparison of the results obtained with the simulation using a single plate and the experimental data, represented by the orange circles, collected (a) on 25 March and (b) on 20 April. The orange and blue lines represent the outlet water temperature obtained with the simulation and the inlet water temperature, respectively.

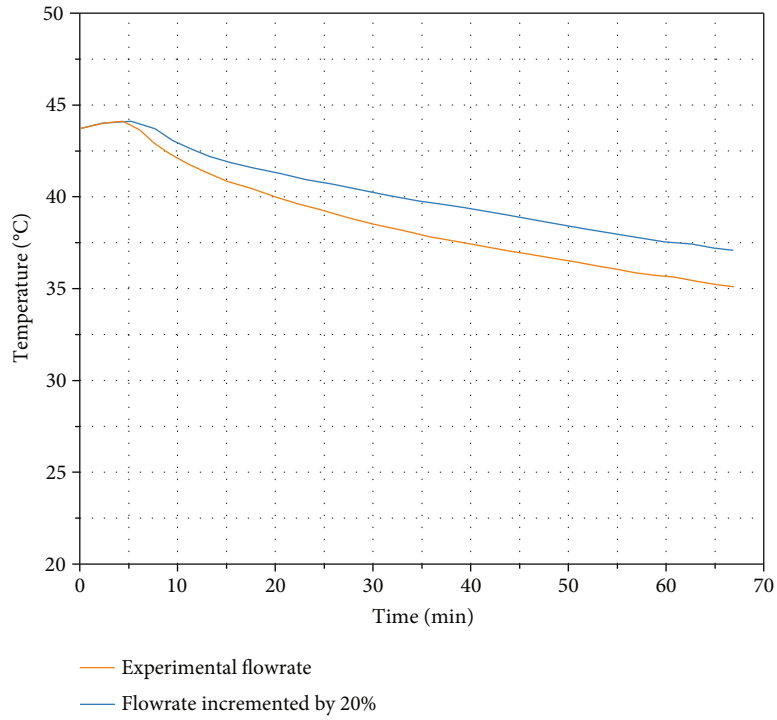

Figure 8: Effect of HTF flow rate during the discharging of the thermal storage.

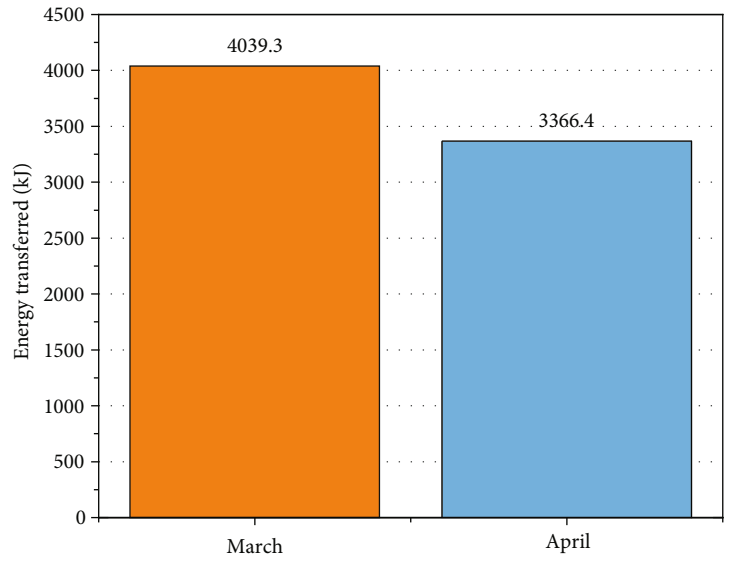

Figure 9: Effect of HTF temperature during the discharge of the thermal storage.

the PCM, as reported in the article of Singh et al. [26]. One straightforward approach involves enhancing heat transfer between the PCM and the heat transfer fluid (HTF) by acting on the convective heat transfer coefficient. This parameter can be increased by adjusting the flow rate of the HTF. Increasing the inlet velocity of HTF enhances the heat transfer rate. However, it reduces the difference between the inlet and outlet temperature of the HTF which reduces the energy stored in the PCM [24]. Several authors studied the effect of mass flow rate on the solidification and melting process of PCM. Sari and Kaygusuz studied the effect of Reynolds number on PCM melting and solidification. They showed that by duplicating the Reynolds number, the melting time was reduced by 23% while the solidification time was reduced by 16% [27]. Different authors show that this effect is more pronounced for melting than solidification [24–28]. Here, to observe the effect of the heat transfer fluid flow rate on the thermal performance of the LHTTS during the discharging process, an additional simulation was performed using the same boundary condition adopted to reproduce the experiment performed in March, with the only variation being a 20% increase in the flow rate of the inlet water. The

initial PCM temperature was assumed to be constant at 47°C; moreover, it was assumed that at $t = 0$, the PCM was completely melted. The temperature profile of the outlet water for the two simulations is shown in Figure 8.

It is observed that during the initial phase, the curves are nearly coincident, and the maximum temperature difference between the two curves is 5%. This is consistent with findings in other studies in the literature, as reported by Seddegh et al. [29]. This phenomenon can be explained by the primary thermal resistance being on the phase change material side. Therefore, the reduction of thermal resistance on the HTF side, resulting from the increased flow rate, has a comparatively lower impact on heat transfer.

4.2.2. Variation of the HTF Temperature. Different articles showed that in LTHSS systems, the HTF inlet temperature substantially affects the heat transfer rate [30–32]. An increase in the difference between the phase change temperature of the PCM and the temperature of the inlet HTF results in a reduction of the total solidification time.

To evaluate the effect of this parameter, the temperatures obtained from the two simulations using inlet temperature recorded in March and April were used to calculate the thermal energy released in two hours using the following relationships:

$$Q_i = \dot{m}_{H_2O} c_p (T_{out,i} - T_{in,i}) \Delta t,$$
$$Q_{tot} = \sum_{t_{in}}^{t_{fin}} Q_i, \quad (12)$$

where Δt represents the time interval between one measurement and the following one. Considering the March experimental data over two hours and the maximum temperature difference between the inlet water temperature and the phase change temperature of the PCM, a maximum value of 21.5°C and an average value of 14.9°C are obtained. Considering the second set of experimental data collected in April, a maximum value of 21°C and an average value of 8.9°C were obtained. On average, the observed temperature difference in April is lower by a factor of 0.6 than in March. Figure 9 shows the amount of thermal energy released during the discharge phase of the LHTSS over a 2-hour period. The amount of energy released in March is higher than in April, confirming that a greater temperature difference corresponds to a higher rate of heat transfer and, consequently, a faster release of thermal energy. This agrees with the numerical and experimental study conducted in [31].

5. Conclusion

This study explored the integration of a latent heat storage system with an air-water heat pump to improve energy efficiency during periods of low demand. The configuration, with a heat exchanger for thermal energy storage in series with the heat pump, has shown promising results, allowing the heat pump to operate at rated conditions and storing excess thermal energy in a PCM system. This stored energy can be efficiently integrated to produce domestic hot water and heating, as required. The model developed in this work has proven effective in predicting the discharge processes of the PCM storage system and is a valuable tool for optimizing heat exchanger design. In addition, changes in the flow rate and temperature of the heat transfer fluid were analysed. A greater temperature difference between the melting temperature of the PCM and the inlet temperature of the HTF had a greater impact on the heat transfer, while increasing the HTF flow rate had less influence on the exhaust process. Overall, the results suggest that integrating LHTSS with heat pumps can improve overall system performance, achieve energy savings, and provide a more sustainable approach to thermal energy management.

Nomenclature

CFD: Computational fluid dynamics
COP: Coefficient of performance
HTF: Heat transfer fluid
LHTSS: Latent heat thermal storage system
PCMs: Phase change materials.

Units of measure

c_p: Specific heat (J/(kg•K))
$c_{p,app}$: PCM apparent heat capacity (J/(kg•K))
k: Thermal conductivity (W/(m•K))
m_{PCM}: Mass of phase change material (kg)
$\dot{m}_{H_2O}$: Water fluid mass flow rate (kg/s)
p: Heat transfer fluid pressure (Pa)
Q_i: Exchanged thermal energy at i-th time instant (kJ)
Q_{tot}: Total exchanged thermal energy (kJ)
T: Temperature (°C)
t: Time (s)
$T_{in,i}$: Heat transfer fluid inlet temperature at i-th time instant (°C)
$T_{out,i}$: Heat transfer fluid outlet temperature at i-th time instant (°C)
V_{PCM}: Volume of phase change material (m^3).

Symbols

Δt: Time interval (s)
Λ: PCM latent heat (J/kg)
μ: Heat transfer fluid dynamic viscosity (Pa•s)
ρ: Density (kg/m^3)
ρ_l: PCM density in the liquid phase (kg/m^3)
ρ_s: PCM density in the solid phase (kg/m^3).

Data Availability

Data will be submitted on request.

Disclosure

The work presented here is derived from the work developed by the first author, Piera Di Prima, and presented as an Energy Engineering thesis at the Polytechnic University of Turin.

Conflicts of Interest

The authors declare that they have no conflicts of interest.

References

[1] IEA, *Renewables 2019*, IEA, Paris, 2019, https://www.iea.org/reports/renewables-2019.

[2] C. Yang, S. Seo, N. Takata, K. Thu, and T. Miyazaki, "The life cycle climate performance evaluation of low-GWP refrigerants for domestic heat pumps," *International Journal of Refrigeration*, vol. 121, pp. 33–42, 2021.

[3] P. Moreno, C. Solé, A. Castell, and L. F. Cabeza, "The use of phase change materials in domestic heat pump and air-conditioning systems for short term storage: a review," *Renewable and Sustainable Energy Reviews*, vol. 39, pp. 1–13, 2014.

[4] S. Rashidi, H. Shamsabadi, J. A. Esfahani, and S. Harmand, "A review on potentials of coupling PCM storage modules to heat pipes and heat pumps," *Journal of Thermal Analysis and Calorimetry*, vol. 140, pp. 1655–1713, 2020.

[5] A. Pignata, F. D. Minuto, A. Lanzini, and D. Papurello, "A feasibility study of a tube bundle exchanger with phase change materials: a case study," *Journal of Building Engineering*, vol. 78, article 107622, 2023.

[6] W. Youssef, Y. T. Ge, and S. A. Tassou, "CFD modelling development and experimental validation of a phase change material (PCM) heat exchanger with spiral-wired tubes," *Energy Conversion and Management*, vol. 157, pp. 498–510, 2018.

[7] E. Assis, G. Ziskind, and R. Letan, "Numerical and experimental study of solidification in a spherical shell," *Journal of Heat Transfer*, vol. 131, no. 2, 2009.

[8] S. D. Proell, C. Meier, and W. A. Wall, "Accuracy and performance of phase change and latent heat models in metal additive manufacturing process simulation," 2019, https://deepai.org/publication/accuracy-and-performance-of-phase-change-and-latent-heat-models-in-metal-additive-manufacturing-process-simulation.

[9] J. H. Nazzi Ehms, R. De Césaro Oliveski, L. A. Oliveira Rocha, C. Biserni, and M. Garai, "Fixed grid numerical models for solidification and melting of phase change materials (PCMs)," *Applied Sciences*, vol. 9, no. 20, p. 4334, 2019.

[10] R. V. Wilson, F. Stern, H. W. Coleman, and E. G. Paterson, "Comprehensive approach to verification and validation of CFD simulations—part 2: application for RANS simulation of a cargo/container ship," *Journal of Fluids Engineering*, vol. 123, no. 4, pp. 803–810, 2001.

[11] K. Piechurski, M. Szulgowska-Zgrzywa, and J. Danielewicz, "The impact of the work under partial load on the energy efficiency of an air-to-water heat pump," *E3S Web of Conferences*, vol. 17, article 00072, 2017.

[12] G. Zsembinszki, A. G. Fernández, and L. F. Cabeza, "Selection of the appropriate phase change material for two innovative compact energy storage systems in residential buildings," *Applied Sciences*, vol. 10, no. 6, p. 2116, 2020.

[13] M. M. Farid, A. M. Khudhair, S. A. K. Razack, and S. Al-Hallaj, "A review on phase change energy storage: materials and applications," *Energy Conversion and Management*, vol. 45, no. 9-10, pp. 1597–1615, 2004.

[14] G. Yang, Y. J. Yim, J. W. Lee, Y. J. Heo, and S. J. Park, "Carbon-filled organic phase-change materials for thermal energy storage: a review," *Molecules*, vol. 24, no. 11, p. 2055, 2019.

[15] S. G. Jeong, O. Chung, S. Yu, S. Kim, and S. Kim, "Improvement of the thermal properties of bio-based PCM using exfoliated graphite nanoplatelets," *Solar Energy Materials and Solar Cells*, vol. 117, pp. 87–92, 2013.

[16] Phase Change Energy Solutions, *Bio PCM Q42 technical data*, Asheboro, NC 27203, USA, 2022.

[17] G. Triscari, M. Santovito, M. Bressan, and D. Papurello, "Experimental and model validation of a phase change material heat exchanger integrated into a real building," *International Journal of Energy Research*, vol. 45, no. 12, pp. 18222–18236, 2021.

[18] J. Stefan, "Uber einge problem der theoric der warmeleitung, sb wein," *Academic Matters Nature*, vol. 98, pp. 173–484, 1989.

[19] M. Turkyilmazoglu, "Stefan problems for moving phase change materials and multiple solutions," *International Journal of Thermal Sciences*, vol. 126, pp. 67–73, 2018.

[20] H. Hu and S. A. Argyropoulos, "Mathematical modelling of solidification and melting: a review," *Modelling and Simulation in Materials Science and Engineering*, vol. 4, no. 4, pp. 371–396, 1996.

[21] Y. Belhamadia, A. S. Kane, and A. Fortin, "An enhanced mathematical model for phase change problems with natural convection," *International Journal of Numerical Analysis and Modeling*, vol. 3, no. 2, pp. 192–206, 2012, http://www.math.ualberta.ca/ijnamb/Volume-3-2012/No-2-12/2012-02-05.pdf.

[22] M. J. Zarei, H. Bazai, M. Sharifpur, O. Mahian, and B. Shabani, "The effects of fin parameters on the solidification of PCMs in a fin-enhanced thermal energy storage system," *Energies*, vol. 13, no. 1, p. 198, 2020.

[23] H. Coleman and Members, Committee, *ASME V & V 20-2009 standard for verification and validation in computational fluid dynamics and heat transfer*, Elsevier, 2009.

[24] L. Kalapala and J. K. Devanuri, "Influence of operational and design parameters on the performance of a PCM based heat exchanger for thermal energy storage–a review," *Journal of Energy Storage*, vol. 20, pp. 497–519, 2018.

[25] N. P. Tsolakoglou, M. K. Koukou, M. G. Vrachopoulos, N. Tachos, K. Lymberis, and V. Stathopoulos, "Experimental process investigation of a latent heat energy storage system with a staggered heat exchanger with different phase change materials for solar thermal energy storage applications," *E3S Web of Conferences*, vol. 22, article 00179, 2017.

[26] R. Singh, S. Sadeghi, and B. Shabani, "Thermal conductivity enhancement of phase change materials for low-temperature thermal energy storage applications," *Energies*, vol. 12, no. 1, p. 75, 2019.

[27] A. Sari and K. Kaygusuz, "Thermal performance of a eutectic mixture of lauric and stearic acids as PCM encapsulated in the annulus of two concentric pipes," *Solar Energy*, vol. 72, no. 6, pp. 493–504, 2002.

[28] Y. Wang, L. Wang, N. Xie, X. Lin, and H. Chen, "Experimental study on the melting and solidification behavior of erythritol in a vertical shell-and-tube latent heat thermal storage unit," *International Journal of Heat and Mass Transfer*, vol. 99, pp. 770–781, 2016.

[29] S. Seddegh, X. Wang, M. M. Joybari, and F. Haghighat, "Investigation of the effect of geometric and operating parameters on thermal behavior of vertical shell-and-tube latent heat energy storage systems," *Energy*, vol. 137, pp. 69–82, 2017.

[30] B. Lamrani, A. Khouya, and A. Draoui, "Numerical modelling of a latent heat thermal energy storage system applied to solar

drying techniques," *International Journal of Energy, Environment and Economics*, vol. 25, no. 2, pp. 153–167, 2017.

[31] F. Benmoussa, A. Benzaoui, and H. Benmoussa, "Thermal behavior of latent thermal energy storage unit using two phase change materials: effects of HTF inlet temperature," *Case Studies in Thermal Engineering*, vol. 10, pp. 475–483, 2017.

[32] W. W. Wang, K. Zhang, L. B. Wang, and Y. L. He, "Numerical study of the heat charging and discharging characteristics of a shell-and-tube phase change heat storage unit," *Applied Thermal Engineering*, vol. 58, no. 1-2, pp. 542–553, 2013.